



## Noninvasive, *in vivo* assessment of the cervical microcirculation using incident dark field imaging

Yani P. Latul<sup>a,\*</sup>, Arnoud W. Kastelein<sup>a</sup>, Patricia W.T. Beemster<sup>b</sup>, Nienke E. van Trommel<sup>c</sup>, Can Ince<sup>d</sup>, Jan-Paul W.R. Roovers<sup>a,b</sup>

<sup>a</sup> Amsterdam UMC, University of Amsterdam, Department of Obstetrics and Gynaecology, Amsterdam Reproduction & Development Research Institute, Meibergdreef 9, 1105 AZ Amsterdam, the Netherlands

<sup>b</sup> Bergman Clinics, Department of Gynaecology, Bergman Vrouwenzorg, Nijenburg 152, 1081 GG Amsterdam, the Netherlands

<sup>c</sup> Center for Gynecologic Oncology Amsterdam, Location Antoni van Leeuwenhoek Hospital/The Netherlands Cancer Institute, Plesmanlaan 121, 1066CX Amsterdam, the Netherlands

<sup>d</sup> Erasmus Medical Center, Department of Intensive Care, Laboratory of Translational Intensive Care, Doctor Molewaterplein 40, 3015 GD Rotterdam, the Netherlands

### ARTICLE INFO

#### Keywords:

Microcirculation  
IDF imaging  
Microvessel density  
Capillary density  
Angioarchitecture  
Uterine cervix

### ABSTRACT

**Aim:** This study evaluates the feasibility of handheld vital microscopy for noninvasive, objective assessment of the microcirculation of the human uterine cervix. We qualitatively and quantitatively describe the microcirculation in healthy subjects in order to provide a basis for its application in cervical pathology.

**Methods:** Incident dark field imaging was used to image the microcirculation in four quadrants of the uterine ectocervix in ten healthy participants. If the squamocolumnar junction was visible, measurements were repeated on the endocervical columnar epithelium as well. Image acquisition time was recorded and participants scored the experienced level of discomfort. Angioarchitecture was classified according to Weber's classification. Quantitative parameters included capillary density (CD), total and perfused vessel density (TVD, PVD), proportion of perfused vessels (PPV) and microvascular flow index (MFI).

**Results:** Image acquisition was easy, fast and well tolerated. Angioarchitecture was characterized by two distinctive and organized patterns; capillary loops underneath the squamous epithelium of the ectocervix and vascular networks underneath the columnar epithelium. In the image sequences containing capillary loops, mean CD was 33.2 cpl/mm<sup>2</sup> (95% CI 28.2–38.2 cpl/mm<sup>2</sup>). In the image sequences with vascular networks, mean TVD was 12.5 mm/mm<sup>2</sup> (95% CI 11.2–13.77 mm/mm<sup>2</sup>), mean PVD was 12.2 (95% CI 11.0–13.5 mm/mm<sup>2</sup>), MFI was 3 and PPV was 100%.

**Conclusions:** Incident dark field imaging allows for noninvasive, real time visualization and objective evaluation and quantification of the microcirculation of the uterine cervix. The organized vascular patterns and optimal perfusion observed in healthy subjects allow for comparison with cervical pathology, for example in patients with cervical dysplasia or cervical cancer.

### 1. Introduction

The uterine cervix is the cylindrically shaped, inferior portion of the uterus which protrudes into the upper part of the vagina and connects the uterine cavity to the vaginal lumen through the cervical canal (Ferenczy and Wright, 1994; Hoare and Khan, 2020). It is involved in physiological processes including fertilization, pregnancy, childbirth and menstruation and provides a barrier for pathogens of the upper

female reproductive tract (Jordan and Singer, 2006). The vascularization of the uterine cervix is derived from both the uterine and vaginal artery, of which terminal branches anastomose to form the coronary artery of the cervix (Krantz and Phillips, 1962).

Within tissues, the regulation of perfusion and hence the supply of oxygen, nutrients, hormones and immune support and the drainage of waste products, takes place in the arterioles, capillaries and venules, together referred to as the microcirculation (Eriksson et al., 2014; Guven

**Abbreviations:** CD, capillary density; IDF, incident dark field; MFI, microvascular flow index; PPV, proportion of perfused vessels; PVD, perfused vessel density; SCJ, squamocolumnar junction; TVD, total vessel density.

\* Corresponding author.

E-mail address: [y.p.latul@amsterdamumc.nl](mailto:y.p.latul@amsterdamumc.nl) (Y.P. Latul).

<https://doi.org/10.1016/j.mvr.2021.104145>

Received 15 January 2021; Received in revised form 3 February 2021; Accepted 4 February 2021

Available online 9 February 2021

0026-2862/© 2021 The Author(s). Published by Elsevier Inc. This is an open access article under the CC BY license (<http://creativecommons.org/licenses/by/4.0/>).

et al., 2020). By regulating the exchange of fluids and molecules, the microcirculation is responsible for tissue homeostasis and consequently tissue wellness (Guven et al., 2020). Accordingly, the microcirculation plays a crucial role in many pathological processes, including inflammation, sepsis, shock and tumor growth (Bouck et al., 1996; Guven et al., 2020).

Likewise, the microcirculation of the uterine cervix is involved in its immune and tissue response to physiological and pathological conditions, including cervical ripening, cervicitis, infection with human papillomavirus, cervical dysplasia and cancer (Abdullaiev et al., 2017; Agrawal et al., 2020; Chen et al., 2004; D'Anna et al., 2001; Dunlop et al., 1989; Jourdan et al., 2011; Sotiropoulou et al., 2004).

In daily practice, the (micro)vasculature of the uterine cervix is either assessed macroscopically and subjectively by colposcopy or invasively by biopsies. Noninvasive, objective imaging of the cervical microcirculation offers an opportunity for real time assessment of functional vascular histology, which may improve diagnosis and understanding of cervical pathology, and possibly also guide treatment strategies. For example, predicting malignant potential of cervical cancer precursor lesions based on histology and colposcopy is difficult, which in turn makes management decisions (expectant or surgery) challenging (Cox, 2002). An alternative method that improves insight in malignant potential is therefore desirable.

In different fields of medicine, *in vivo* assessment of the microcirculation is of increasing interest. Incident dark field (IDF) imaging is a noninvasive handheld vital microscope that enables visualization of the (sub)epithelial microcirculation in great detail (Aykut et al., 2015). Consequently, IDF imaging has provided insight in microcirculatory alterations in both systemic and organ specific pathological conditions (de Bruin et al., 2016; Diedrich et al., 2019; Edul et al., 2012; Kastelein et al., 2020a, 2020b; Puhl et al., 2003; Shen et al., 2020; Uz et al., 2019; van Elteren et al., 2015; Vellinga et al., 2015). IDF imaging has not yet been used to evaluate the microcirculation of the uterine cervix.

This study assesses the feasibility of IDF imaging for qualitative and quantitative evaluation of the subepithelial microcirculation of the uterine cervix and provides baseline microcirculatory values of healthy women against which pathological abnormalities can be evaluated in future studies.

## 2. Methods

This observational prospective pilot study was performed in Bergman Clinics Amsterdam, a clinic focusing on pelvic floor care and premalignant cervical lesions. The study complied with ethical principles and appropriate regulatory requirements of the European Union and the Netherlands. As part of a comprehensive study on microvascular alterations in cervical cancer and precursor lesions, the protocol was reviewed and approved by the Institutional Review Board of the Antoni van Leeuwenhoek Hospital under number METC18.0773 and locally approved by Bergman Clinics Amsterdam. Participants received verbal and written explanation of the study guidelines and procedures and provided written informed consent.

### 2.1. Participants and setting

Healthy, female volunteers (age 18 years and older) attending Bergman Clinics were recruited. Characteristics including age, smoking status and BMI were registered. Exclusion criteria were: 1. diagnosed cervical abnormalities (cervical intraepithelial neoplasia, invasive cervical cancer), 2. prior interventions to the cervix (biopsy, loop excision, exconization), 3. extensive cardiovascular disease (e.g. untreated hypertension), 4. systemic illnesses which may affect the microcirculation (e.g. untreated diabetes mellitus) and 5. medications which may affect the microcirculation (e.g. anticoagulants, systemic anti-inflammatory, or immunosuppressive agents).

### 2.2. Incident dark field imaging

The microcirculation was assessed using the CytoCam (Braedius Medical, Huizen, the Netherlands), which is a lightweight, handheld vital microscope (HVM) which uses the technique of incident dark field imaging. This technique has been described extensively elsewhere (De Backer et al., 2007; Ocak et al., 2016). In short, put into contact with a surface, the CytoCam illuminates the target tissue by emitting green light (wavelength 530 nm) with a short pulse time (2 ms). The green light is absorbed by hemoglobin, scattered back by the surrounding tissues and detected by a camera containing a high-resolution sensor (pixel size 1,4  $\mu\text{m}$ , magnification factor 4 $\times$ ), resulting in real time visualization of flowing black globules (erythrocytes) in white surroundings (avascular tissue) in a field of view of 1,16  $\times$  1,55 mm, representing the functional microcirculation.

### 2.3. Image acquisition

Participants were accommodated in a gynaecological chair in a room with a constant temperature of 21  $\pm$  1  $^{\circ}\text{C}$ . Measurements were performed in lithotomy position. A lubricated, disposable, bivalved speculum was introduced vaginally, the cervix was visualized and cleared from mucus and lubricant. The CytoCam was covered with a sterile disposable cap and gently placed onto the surface of the cervix. The settings of the CytoCam were adjusted for optimal focus and contrast. Artefacts caused by excessive mucus or air bubbles were resolved by clearing the cervical surface from mucus and gently twisting the probe. In four quadrants of the cervix (at 12, 3, 6 and 9 o'clock), an image sequence of 3 s was recorded. If the squamocolumnar junction (SCJ) was visible, measurements were repeated in the same four quadrants on the columnar epithelium at the start of the endocervix as well. Measurements were performed by one investigator (YPL), trained by a researcher with extensive experience using the CytoCam (AWK). As a measure of practical feasibility, total time of image acquisition was recorded and participants were asked to score the level of discomfort they experienced during measurements on a scale of 0 to 10 (0 = none, 10 = extreme).

### 2.4. Image sequence analysis

Acquired image sequences were saved on a hard drive and image analysis was performed offline. The quality of each image sequence was assessed through a quality score, which includes six parameters: illumination, duration, focus, content, stability and pressure (Massey and Shapiro, 2016). As we did not want to exclude image sequences containing capillary loops only, we adapted the parameter 'content' to artefacts only. If an image sequence did not meet the other parameters, it was excluded from further analysis.

#### 2.4.1. Angioarchitecture

Image sequences were scored according to a classification introduced by Weber et al. (2015), which classifies vascular patterns in scores 1 to 3 (Weber et al., 2015). In this classification system, score 1 represents the appearance of an array of capillary loops, score 2 the appearance of both capillary loops and vascular network and score 3 the appearance of a vascular network only, without capillary loops. The angioarchitecture of each image sequence was evaluated and scored manually by one investigator (YPL), trained and supervised by an investigator with extensive experience using this scoring system (AWK). As capillary loops and vascular networks require different approaches for quantitative analysis, image sequences with angioarchitecture score 2 were excluded from quantitative analysis.

#### 2.4.2. Quantifying capillary loops

In case of angioarchitecture score 1, the capillary loop density (CD, capillary loops per square millimeter; cpil/mm<sup>2</sup>) was determined by dividing the number of capillary loops by the size of the field of view

(1,8 mm<sup>2</sup>).

### 2.4.3. Quantifying vascular networks

In image sequences containing angioarchitecture score 3, quantitative microvascular parameters were evaluated using Automated Vascular Analysis (AVA) software v3.2 (Dobbe et al., 2008). Using this software, the frame of the recorded image sequences was stabilized and vessels were detected semi-automatically. After manual correction of detected vessels, the flow within each vessel was scored by eye as no flow (0), intermittent flow (1), sluggish flow (2) or continuous flow (3) (Massey and Shapiro, 2016). The predominant type of flow was determined in four quadrants. Subsequently, total vessel density (TVD, total length of vessels per square millimeter, mm/mm<sup>2</sup>), perfused vessel density (PVD, perfused vessels per square millimeter, mm/mm<sup>2</sup>), proportion of perfused vessels (PPV, %) and microvascular flow index (MFI) were determined (Aykut et al., 2015).

### 2.5. Sample size calculation

We did not perform a sample size calculation but determined a convenient sample of ten participants sufficient for this explorative pilot study. A previous study performed in nine healthy volunteers concluded that the vaginal microcirculation can be assessed reliably using IDF imaging in a small sample (Weber et al., 2015).

### 2.6. Statistical analysis

Demographic and microcirculation data were analyzed using IBM SPSS Statistics (IBM Corp. Released 2020. IBM SPSS Statistics for Macintosh, Version 27.0. Armonk, NY: IBM Corp). Categorical data regarding angioarchitecture are presented as absolute and relative frequencies. Distributions of observed angioarchitectures were compared between cervical locations using the Chi square test. Continuous data were tested for normality both visually and using the Shapiro-Wilk test. Normally distributed data are presented as means and 95% confidence intervals (95% CI). Non-normally distributed data are presented as medians and interquartile ranges (IQR). Spearman's correlation was analyzed to assess the relationship between age and CD, TVD and PVD. A two-sided *p*-value below 0.05 was considered to be the threshold for statistical significance.

## 3. Results

### 3.1. Description of population and obtained data

Measurements were performed in ten healthy participants with a median age of 32 years [27–74] and mean BMI of 22.4 [20.8–23.9]. One of the participants occasionally smoked. None of the participants had relevant comorbidity. All participants above 30 years of age participated in the Dutch national screening program and did not have prior cervical dysplasia. No recent Pap status was known for the participants outside of the screening window (30–60 years of age). However, no signs or symptoms of cervical pathology were present in these participants. Upon physical examination of the ectocervix, five subjects revealed only squamous epithelium. In four subjects, the SCJ was visible, allowing for image acquisition of both squamous and columnar epithelium. In one subject, the SCJ was visible at the border of the ectocervix, but the squamous epithelium was not accessible for IDF measurements. A total of 56 IDF image sequences were recorded of which seven were excluded from analysis of angioarchitecture because of poor image quality (excessive vaginal discharge blurring the image) and two were excluded because they were recorded at the SCJ, leaving 47 image sequences (31 of squamous epithelium, 16 of columnar epithelium) for the analysis of angioarchitecture. For quantitative analysis of microcirculatory parameters, three more image sequences had to be excluded because of an angioarchitecture score of 2.

### 3.2. Feasibility

Image acquisition was convenient and well tolerated; all subjects scored their level of discomfort 0 to 2 out of 10 (0 = none, 10 = extreme). Image acquisition time ranged from 2 to 6 min and was dependent on the number of image sequences recorded; if the SCJ was visible, more image sequences were recorded and image acquisition time was longer.

### 3.3. Angioarchitecture

Acquired image sequences demonstrated very distinct and organized vascular patterns that could all be classified according Weber's classification. In general, the microcirculation of the ectocervix was characterized by capillary loops (71% score 1, Figs. 1 and 4) and the microcirculation of the columnar epithelium at the start of the endocervix predominantly showed a vascular network (88% score 3, Figs. 2 and 4). At the SCJ, a transition area of both patterns could be observed (100% score 2, Fig. 3). The proportions of the observed angioarchitectures were significantly different between the squamous and columnar epithelium ( $\chi^2$  (2, *n* = 47) = 19.0, *p* < 0.01, Fig. 4). Sub-analysis of angioarchitecture scores in the four patients in which image sequences could be obtained of both squamous and columnar epithelium demonstrated similar distributions of proportions ( $\chi^2$  (2, *n* = 25) = 11.7, *p* < 0.01, Fig. 4).

### 3.4. Microcirculatory parameters

Shapiro-Wilk testing for normality showed normal distributions for CD, TVD and PVD and non-normal distributions for MFI and PPV. Mean CD calculated from image sequences demonstrating capillary loops only (score 1, *n* = 23), was 33.2 cpl/mm<sup>2</sup> [28.2–38.2]. There was no correlation between age and mean CD (*r* = -0.095, *p* = 0.82). In image sequences containing vascular networks (score 3, *n* = 21), mean TVD was 12.5 mm/mm<sup>2</sup> [11.2–13.8] and mean PVD was 12.2 [11.0–13.5]. Age did not correlate with TVD (*r* = 0.458, *p* = 0.30). Continuous flow was observed in all visualized vessels, resulting in a median MFI of 3 [3–3] and a median PPV of 100% [100–100].

## 4. Discussion

The results of this study suggest that *in vivo* imaging of the microcirculation of the uterine cervix using IDF imaging is feasible. Image acquisition was fast, easy and well tolerated by all participants and resulted in image sequences that could be qualitatively and quantitatively analyzed. Two distinct and organized vascular patterns were observed: capillary loops at the squamous epithelium and vascular networks at the columnar epithelium. Optimal perfusion was observed in all recorded image sequences.

The uterine cervix is lined with two types of epithelium; stratified, squamous epithelium on the ectocervix and a single layer of columnar epithelium on the endocervix (Dallenbach-Hellweg et al., 2013). *Ex vivo* studies of the microcirculation of the uterine cervix using corrosion casting and scanning electron microscopy revealed four zones with different vascular patterns within the cervical stroma, but were unable to evaluate the microcirculation of the cervical epithelium as it was too fragile for this technique (Bereza et al., 2012a, 2012b; Walocha et al., 2012). The squamous epithelium on the ectocervix is continuous with the squamous epithelium of the vagina. Weber et al. (2015) have visualized the microcirculation of the vagina *in vivo* through sidestream dark field imaging, the predecessor of IDF imaging, and described the appearance of capillary loops as well (Weber et al., 2015). As expected, our results predominantly demonstrated the same angioarchitecture in the squamous epithelium lining the ectocervix. We also observed similar CD within this epithelium when compared to vaginal CD described before (Weber et al., 2015, 2016). Another study using IDF imaging in

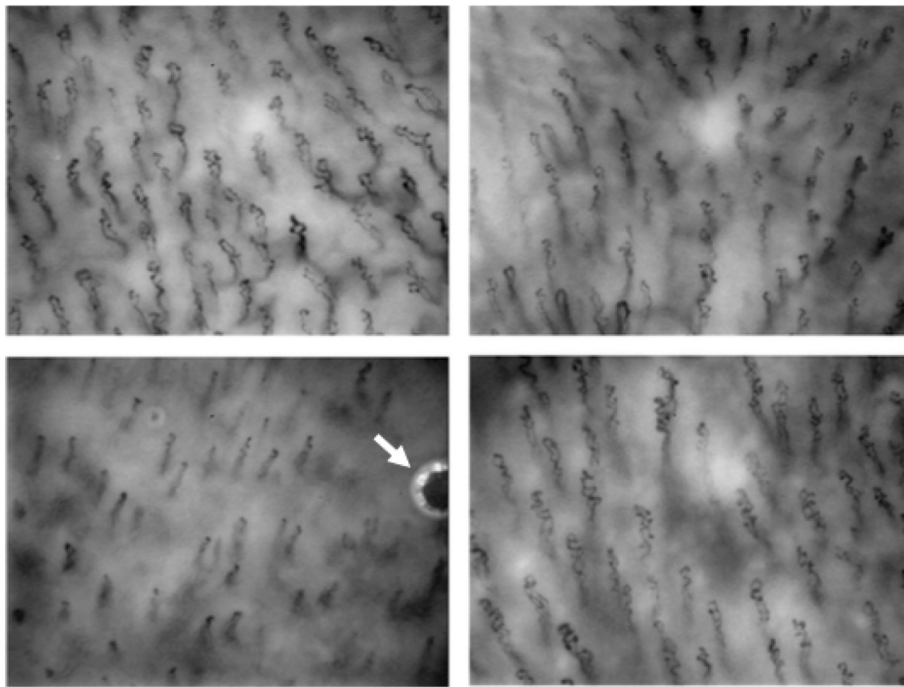


**Fig. 1.** Screenshots of IDF imaging of the squamous epithelium of four different participants showing angioarchitecture score 1 (capillary loops only). White arrow labels artefact (bubble).

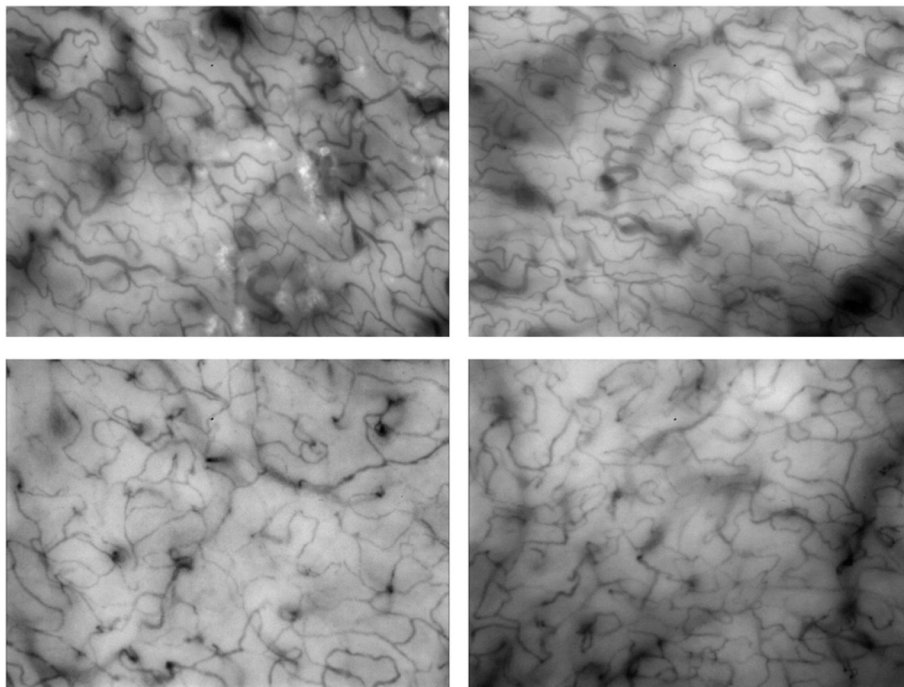


**Fig. 2.** Screenshots of IDF imaging of the columnar epithelium of four different participants showing angioarchitecture score 3 (vascular networks without capillary loops).

vulvovaginal atrophy demonstrated that thinning of vaginal epithelium (atrophy) corresponds with disappearance of vaginal loops and appearance of vascular networks (Diedrich et al., 2019). In the current study, we did not assess atrophic epithelium, but we did assess two types of epithelium with different thicknesses and also demonstrated the presence of vascular networks underneath the thinner – in our case columnar – epithelium and capillary loops underneath the thicker, stratified squamous epithelium. Capillary density of the atrophic vaginal

epithelium was much lower when compared to CD we observed in the ectocervix (Diedrich et al., 2019). Quantitative microcirculatory parameters of vascular networks (score 3, including TVD, PVD, PPV) have not been described in the vagina yet. Compared to the golden standard of sublingual microcirculatory assessment, the uterine cervix has a lower TVD (Uz et al., 2018).

Our study demonstrated that IDF imaging enables noninvasive objective evaluation of the cervical microcirculation. The two distinct,

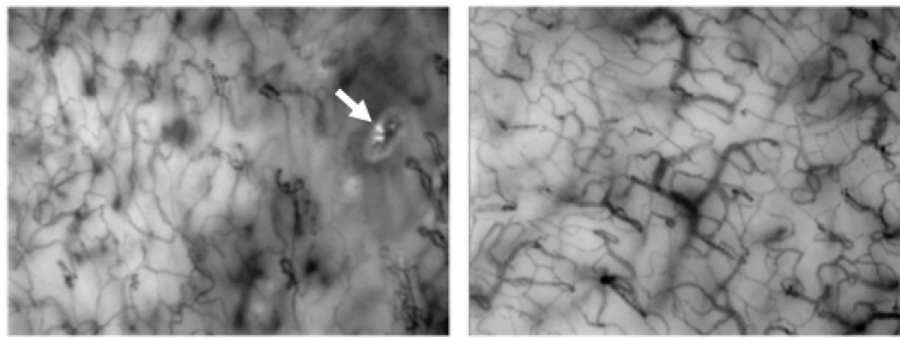


**Fig. 3.** Screenshots of IDF imaging of the squamocolumnar junction, showing angioarchitecture score 2 (both vascular networks and capillary loops). White arrow labels artefact (bubble).

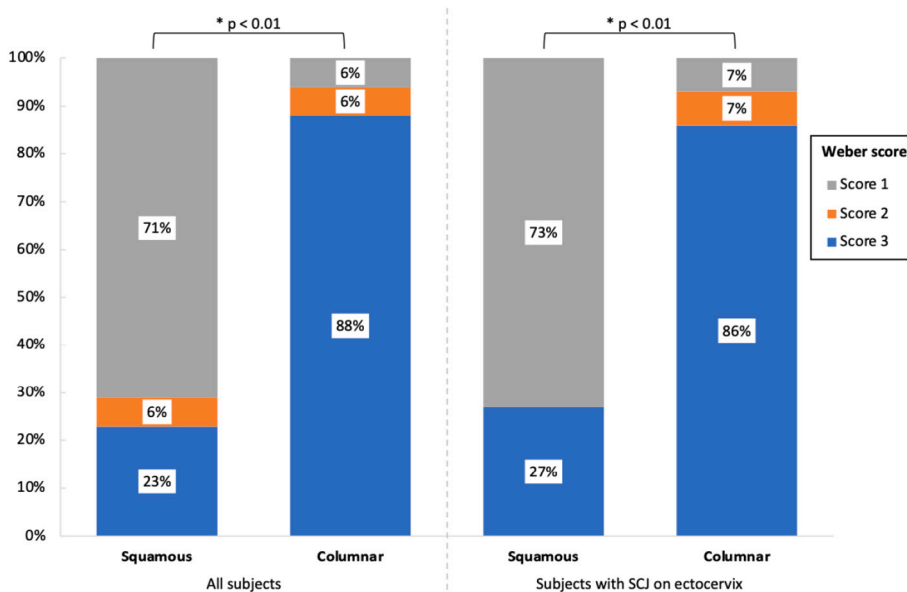


**Fig. 4.** Stacked bar chart presenting observed angioarchitecture scores according to Weber's classification on squamous and columnar epithelium of the cervix. Left: image sequences of all subjects on squamous epithelium (total  $n = 31$ , score 1: 71% ( $n = 22$ ), score 2: 6% ( $n = 2$ ), score 3: 23% ( $n = 7$ )) and columnar epithelium (total  $n = 16$ , score 1: 6% ( $n = 1$ ), score 2: 6% ( $n = 1$ ), score 3: 88% ( $n = 14$ )). Right: image sequences of four subjects in which the SCJ was visible upon physical examination on squamous epithelium (total  $n = 11$ , score 1: 73% ( $n = 8$ ), score 2: 0% ( $n = 0$ ), score 3: 27% ( $n = 3$ )) and columnar epithelium (total:  $n = 14$ , score 1: 7% ( $n = 1$ ), score 2: 7% ( $n = 1$ ), score 3: 86% ( $n = 12$ )). SCJ = squamocolumnar junction, score 1: appearance of an array of capillary loops, score 2: both capillary loops and vascular network are visible, score 3: appearance of a vascular network, no capillary loops. \* The  $\chi$  square test,  $p < 0.01$ .

organized vascular patterns observed in healthy participants allow for comparison with pathological conditions of the uterine cervix. Cervical dysplasia, cervical infection and cervical incompetence may be diagnosed by changes in the cervical microcirculation prior to their clinical manifestation. Multiple histopathological studies show gradual microvascular alterations with increasing dysplasia and these alterations have been associated with poor prognosis and higher mortality in cervical cancer patients (Bremer et al., 1996; Dellas et al., 1997; Dobbs et al., 1997; Guidi et al., 1995; Lee et al., 2002; Obermair et al., 1998; Smith-McCune, 1997; Wiggins et al., 1995). Predicting the malignant potential of cervical dysplastic lesions is challenging, which in turn makes adequate management challenging, resulting in *overtreatment* (surgery) of lesions that would regress spontaneously and *undertreatment* (expectant management) with undue concern of low-grade lesions that have the potential to become high grade lesions and ultimately cancer (Orumaa et al., 2019; Rozemeijer et al., 2015; van der Horst et al., 2017). Currently, management decisions are based on cytology and histology (Perkins et al., 2020), but an alternative, more accurate approach for predicting malignant transformation is desirable. Noninvasive evaluation of microvascular alterations could potentially help predict future behavior and thereby guide treatment decisions.

IDF imaging enables imaging of the subepithelial microcirculation of accessible tissues. Therefore, when applied to the uterine cervix, IDF imaging visualizes the superficial microcirculation and not the microcirculation of the cervical stroma. Future research should elucidate

whether microvascular alterations in cervical pathology arise superficially and whether the imaging depth of IDF imaging is sufficient for their evaluation. The squamous epithelium lining the ectocervix was easily accessible through a speculum in all participants and therefore, the subepithelial microcirculation of the ectocervix was easily visualized. However, the columnar epithelium lining the endocervix was only accessible in 4 out of 10 participants enrolled in this study. The SCJ is dynamic and changes its location over time between the cervical canal and the ectocervix, depending on age, hormonal status and pregnancy (Mutter and Prat, 2014). As the probe of the CytoCam is too large for endocervical application, the microcirculation of the columnar epithelium lining the endocervix cannot be evaluated in every woman.

Our explorative feasibility study reports on an innovative approach for *in vivo* evaluation of the cervical microcirculation and presents unique data on both morphological and quantitative microvascular parameters. Potential limitations need to be addressed as well. First, we included a small sample size and as this is the first study applying IDF imaging to the uterine cervix, we could not perform a power calculation. Therefore, it can be debated whether we can generalize our findings to a larger population. We determined a convenient number of 10 participants based on a previous study using IDF imaging on the vaginal epithelium which concluded that the microcirculation could be evaluated reliably in a small sample of 9 subjects (Weber et al., 2015). Second, the field of view of the CytoCam is relatively small ( $1.55 \times 1.16$  mm), which raises the question whether the obtained image sequences are a

good representative of the entire uterine cervix. As we demonstrated very similar, well organized vascular patterns in four quadrants of the uterine cervix, we consider that the image sequences we describe are a good representative of the epithelium imaged. However, when screening for microvascular alterations in case of cervical pathology, a larger field of view would enable more thorough mapping and thereby allow for easier detection of microvascular abnormalities. Last, in the current study, obtained IDF image sequences were analyzed using semi-automated software, which is time-consuming and less practical in the clinical situation. New software called MicroTools has been developed and validated recently, allowing almost 500 times faster and completely automatic analysis (Hilty et al., 2019). Future research should determine whether this software can be used for the analysis of cervical IDF image sequences as well, specifically for the analysis of different patterns such as capillary loops.

The results of our study indicate that IDF imaging is a feasible method for noninvasive, real time visualization and objective evaluation and quantification of the microcirculation of the uterine cervix. The distinct and clearly organized vascular patterns allow for comparison with cervical pathology. Future research should investigate whether pathological conditions of the cervix are associated with microvascular abnormalities that can be detected by IDF imaging.

### Declaration of competing interest

Prof. Ince has developed SDF imaging and is listed as inventor on related patents commercialized by MicroVision Medical (MVM) under a license from Amsterdam University Medical Center (Amsterdam UMC, location AMC). He receives no royalties or benefits from this license. Braedius Medical, a company owned by a relative of Prof. Ince, has developed and designed the CytoCam – a handheld vital microscope using IDF imaging. Prof. Ince has no financial relationship with Braedius Medical of any sort (i.e., has never owned shares or received consultancy or speaker fees from Braedius Medical). Prof. Ince runs an internet site (<https://microcirculationacademy.org>) that offers services (e.g., training, courses, and analysis) related to clinical microcirculation. All other authors declare that they have no conflict of interest.

### Acknowledgements

The authors would like to thank the volunteers that participated in this study and Bergman Clinics for facilitating the study procedures. This research did not receive any specific grant from funding agencies in the public, commercial or not-for-profit sectors. Materials were provided by Braedius Medical (Huizen, the Netherlands). The data that support the findings of this study are available from the corresponding author upon reasonable request.

### Appendix A. Supplementary data

Supplementary data to this article can be found online at <https://doi.org/10.1016/j.mvr.2021.104145>.

### References

Abdullaev, R.Y., Sibihankulov, A.H., Kiriya, D.G., Abdullaev, R.R., 2017. Transvaginal echographic diagnosis of chronic cervicitis. *J. Gynecol. Reprod. Med.* 1.

Agrawal, S., Rezai, H., Buhimschi, C.S., Buhimschi, I.A., Ahmed, A., 2020. Vascular endothelial growth factor (VEGF) promotes cervical ripening in vivo. *Am. J. Obstet. Gynecol.* 222, S169–S170. <https://doi.org/10.1016/j.ajog.2019.11.262>.

Aykut, G., Veenstra, G., Scorcella, C., Ince, C., Boerma, C., 2015. CytoCam-IDF (incident dark field illumination) imaging for bedside monitoring of the microcirculation. *Intensive Care Med.* Exp. 3, 1–10. <https://doi.org/10.1186/s40635-015-0040-7>.

Bereza, T., Tomaszewski, K., Balajewicz-Nowak, M., Mizia, E., Pasternak, A., Walocha, J., 2012a. The vascular architecture of the supravaginal and vaginal parts of the human uterine cervix: a study using corrosion casting and scanning electron microscopy. *J. Anat.* 221, 352–357. <https://doi.org/10.1111/j.1469-7580.2012.01550.x>.

Bereza, T., Tomaszewski, K.A., Walocha, J., Mizia, E., Bachul, P., Chmielewski, P., 2012b. Vascular architecture of the human uterine cervix, as assessed in light- and scanning electron microscopy. *Folia Morphol. (Warsz)* 71, 142–147.

Bouck, N., Stellmach, V., Hsu, S.C., 1996. How tumors become angiogenic. *Adv. Cancer Res.* 69, 135–174.

Bremer, G.L., Tiebosch, A.T., van der Putten, H.W., Schouten, H.J., de Haan, J., Arends, J.W., 1996. Tumor angiogenesis: an independent prognostic parameter in cervical cancer. *Am. J. Obstet. Gynecol.* 174, 126–131.

Chen, W., Li, F., Mead, L., White, H., Walker, J., Ingram, D.A., Roman, A., Mowa, C.N., Jesmin, S., Sakuma, I., Usip, S., Togashi, H., Yoshioka, M., Hattori, Y., Papka, R., Mikhail, M.S., Palan, P.R., Basu, J., Romney, S.L., Yin, R., Peng, Z., Yao, Y., Cao, Z., Lee, J.S., Kim, H.S., Jung, J.J., Lee, M.C., Park, C.S., D'Anna, R., Le Buanec, H., Alessandri, G., Caruso, A., Burny, A., Gallo, R., Zagury, J.F., Zagury, D., D'Alessio, P., 2004. Angiogenesis, cell proliferation and apoptosis in progression of cervical neoplasia. *Hua xi yi ke da xue xue bao = J. West China Univ. Med. Sci. = Huaxi yike daxue xuebao* 30, 176–178, 181. doi:<https://doi.org/10.1016/j.virol.2007.05.030>.

Cox, J.T., 2002. Management of women with cervical cancer precursor lesions. *Obstet. Gynecol. Clin. N. Am.* 29, 787–816. [https://doi.org/10.1016/s0889-8545\(02\)00047-5](https://doi.org/10.1016/s0889-8545(02)00047-5).

Dallenbach-Hellweg, G., von Knebel Doeberitz, M., Trunk-Gemacher, M.J., 2013. *Atlas of Histopathology of the Cervix Uteri*. Springer Science & Business Media.

D'Anna, R., Le Buanec, H., Alessandri, G., Caruso, A., Burny, A., Gallo, R., Zagury, J.F., Zagury, D., D'Alessio, P., 2001. Selective activation of cervical microvascular endothelial cells by human papillomavirus 16-e7 oncoprotein. *J. Natl. Cancer Inst.* 93, 1843–1851.

De Backer, D., Hollenberg, S., Boerma, C., Goedhart, P., Buchele, G., Ospina-Tascon, G., Dobbe, I., Ince, C., 2007. How to evaluate the microcirculation: report of a round table conference. *Crit. Care* 11, R101. <https://doi.org/10.1186/cc6118>.

de Bruin, A.F.J., Kornmann, V.N.N., van der Sloot, K., van Vugt, J.L., Gosselink, M.P., Smits, A., Van Ramshorst, B., Boerma, E.C., Noordzij, P.G., Boerma, D., van Iterson, M., 2016. Sidestream dark field imaging of the serosal microcirculation during gastrointestinal surgery. *Color. Dis. Off. J. Assoc. Coloproctology Gt. Britain Irel.* 18, O103–O110. <https://doi.org/10.1111/codi.13250>.

Dellas, A., Moch, H., Schultheiss, E., Feichter, G., Almendral, A.C., Gudat, F., Torhorst, J., 1997. Angiogenesis in cervical neoplasia: microvessel quantitation in precancerous lesions and invasive carcinomas with clinicopathological correlations. *Gynecol. Oncol.* 67, 27–33. <https://doi.org/10.1006/gyno.1997.4835>.

Diedrich, C.M., Kastelein, A.W., Verri, F.M., Weber, M.A., Ince, C., Roovers, J.-P.W.R., 2019. Effects of topical estrogen therapy on the vaginal microcirculation in women with vulvovaginal atrophy. *Neurourol. Urodyn.* 38, 1298–1304. <https://doi.org/10.1002/nau.23977>.

Dobbe, J.G.G., Streekstra, G.J., Atasever, B., van Zijderdeld, R., Ince, C., 2008. Measurement of functional microcirculatory geometry and velocity distributions using automated image analysis. *Med. Biol. Eng. Comput.* 46, 659–670. <https://doi.org/10.1007/s11517-008-0349-4>.

Dobbs, S.P., Hewett, P.W., Johnson, I.R., Carmichael, J., Murray, J.C., 1997. Angiogenesis is associated with vascular endothelial growth factor expression in cervical intraepithelial neoplasia. *Br. J. Cancer* 76, 1410–1415.

Dunlop, E.M., Garner, A., Darougar, S., Treharne, J.D., Woodland, R.M., 1989. Colposcopy, biopsy, and cytology results in women with chlamydial cervicitis. *Genitourin. Med.* 65, 22–31.

Edul, V.S.K., Enrico, C., Laviolle, B., Vazquez, A.R., Ince, C., Dubin, A., 2012. Quantitative assessment of the microcirculation in healthy volunteers and in patients with septic shock. *Crit. Care Med.* 40, 1443–1448. <https://doi.org/10.1097/CCM.0b013e31823dae59>.

Eriksson, S., Nilsson, J., Stureson, C., 2014. Non-invasive imaging of microcirculation: a technology review. *Med. Devices (Auckl)* 7, 445–452. <https://doi.org/10.2147/MDER.S51426>.

Ferencyz, A., Wright, T.C., 1994. Anatomy and histology of the cervix. In: Kurman, R.J. (Ed.), *Blaustein's Pathology of the Female Genital Tract*. Springer.

Guidi, A.J., Abu-Jawdeh, G., Berse, B., Jackman, R.W., Tognazzi, K., Dvorak, H.F., Brown, L.F., 1995. Vascular permeability factor (vascular endothelial growth factor) expression and angiogenesis in cervical neoplasia. *J. Natl. Cancer Inst.* 87, 1237–1245.

Güven, G., Hilty, M.P., Ince, C., 2020. Microcirculation: physiology, pathophysiology, and clinical application. *Blood Purif.* 49, 143–150. <https://doi.org/10.1159/000503775>.

Hilty, M.P., Guerci, P., Ince, Y., Toraman, F., Ince, C., 2019. MicroTools enables automated quantification of capillary density and red blood cell velocity in handheld vital microscopy. *Commun. Biol.* 2, 217. <https://doi.org/10.1038/s42003-019-0473-8>.

Hoare, B.S., Khan, Y.S., 2020. *Anatomy, Abdomen and Pelvis. Female Internal Genitals*, Treasure Island (FL).

Jordan, J.A., Singer, A., 2006. Chapter 2: the functional anatomy of the cervix, the cervical epithelium and the stroma. In: *The Cervix*. Blackwell Publishing.

Jourdan, P.M., Roald, B., Poggensee, G., Gundersen, S.G., Kjetland, E.F., 2011. Increased vascularity in cervicovaginal mucosa with *Schistosoma haematobium* infection. *PLoS Negl. Trop. Dis.* 5, e1170. <https://doi.org/10.1371/journal.pntd.0001170>.

Kastelein, A.W., Diedrich, C.M., de Waal, L., Ince, C., Roovers, J.-P.W.R., 2020a. The vaginal microcirculation after prolapse surgery. *Neurourol. Urodyn.* 39, 331–338. <https://doi.org/10.1002/nau.24203>.

Kastelein, A.W., Vos, L.M.C., van Baal, J.O.A.M., Koning, J.J., Hira, V.V.V., Nieuwland, R., van Driel, W.J., Uz, Z., van Gulik, T.M., van Rheeën, J., Ince, C., Roovers, J.-P.W.R., van Noorden, C.J.F., Lok, C.A.R., 2020b. Poor perfusion of the microvasculature in peritoneal metastases of ovarian cancer. *Clin. Exp. Metastasis*. <https://doi.org/10.1007/s10585-020-10024-4>.

- Krantz, K.E., Phillips, W.P., 1962. Anatomy of the human uterine cervix, gross and microscopic. *Ann. N. Y. Acad. Sci.* 97, 551–563. <https://doi.org/10.1111/j.1749-6632.1962.tb34666.x>.
- Lee, J.S., Kim, H.S., Jung, J.J., Lee, M.C., Park, C.S., 2002. Angiogenesis, cell proliferation and apoptosis in progression of cervical neoplasia. *Anal. Quant. Cytol. Histol.* 24, 103–113.
- Massey, M.J., Shapiro, N.I., 2016. A guide to human in vivo microcirculatory flow image analysis. *Crit. Care* 20, 35. <https://doi.org/10.1186/s13054-016-1213-9>.
- Mutter, G.L., Prat, J., 2014. *Pathology of the Female Reproductive Tract*, 3rd edition. Churchill Livingstone.
- Obermair, A., Wanner, C., Bilgi, S., Speiser, P., Kaider, A., Reinthaller, A., Leodolter, S., Gitsch, G., 1998. Tumor angiogenesis in stage IB cervical cancer: correlation of microvessel density with survival. *Am. J. Obstet. Gynecol.* 178, 314–319.
- Ocak, I., Kara, A., Ince, C., 2016. Monitoring microcirculation. *Best Pract. Res. Clin. Anaesthesiol.* 30, 407–418. <https://doi.org/10.1016/j.bpa.2016.10.008>.
- Orumaa, M., Leinonen, M.K., Campbell, S., Møller, B., Myklebust, T.Å., Nygård, M., 2019. Recent increase in incidence of cervical precancerous lesions in Norway: Nationwide study from 1992 to 2016. *Int. J. Cancer* 145, 2629–2638. <https://doi.org/10.1002/ijc.32195>.
- Perkins, R.B., Guido, R.S., Castle, P.E., Chelmow, D., Einstein, M.H., Garcia, F., Huh, W. K., Kim, J.J., Moscicki, A.-B., Nayar, R., Saraiya, M., Sawaya, G.F., Wentzensen, N., Schiffman, M., 2020. 2019 ASCCP risk-based management consensus guidelines for abnormal cervical Cancer screening tests and cancer precursors. *J. Low. Genit. Tract Dis.* 24, 102–131. <https://doi.org/10.1097/LGT.0000000000000525>.
- Puhl, G., Schaser, K.D., Vollmar, B., Menger, M.D., Settmacher, U., 2003. Noninvasive in vivo analysis of the human hepatic microcirculation using orthogonal polarization spectral imaging. *Transplantation* 75, 756–761. <https://doi.org/10.1097/01.TP.0000056634.18191.1A>.
- Rozemeijer, K., van Kemenade, F.J., Penning, C., Matthijsse, S.M., Naber, S.K., van Rosmalen, J., van Ballegooijen, M., de Kok, I.M.C.M., 2015. Exploring the trend of increased cervical intraepithelial neoplasia detection rates in the Netherlands. *J. Med. Screen.* 22, 144–150. <https://doi.org/10.1177/0969141315580836>.
- Shen, L., Uz, Z., Verheij, J., Veelo, D.P., Ince, Y., Ince, C., van Gulik, T.M., 2020. Interpatient heterogeneity in hepatic microvascular blood flow during vascular inflow occlusion (Pringle manoeuvre). *Hepatobiliary Surg. Nutr.* 9, 271–283. doi:10.21037/hbsn.2020.02.04.
- Smith-McCune, K., 1997. Angiogenesis in squamous cell carcinoma in situ and microinvasive carcinoma of the uterine cervix. *Obstet. Gynecol.* 89 (3), 482–483.
- Sotiropoulou, M., Diakomanolis, E., Elsheikh, A., Loutradis, D., Markaki, S., Michalas, S., 2004. Angiogenic properties of carcinoma in situ and microinvasive carcinoma of the uterine cervix. *Eur. J. Gynaecol. Oncol.* 25, 219–221.
- Uz, Z., Kastelein, A.W., Milstein, D.M.J., Liu, D., Rassam, F., Veelo, D.P., Roovers, J.-P.W. R., Ince, C., van Gulik, T.M., 2018. Intraoperative incident dark field imaging of the human peritoneal microcirculation. *J. Vasc. Res.* 55, 136–143. <https://doi.org/10.1159/000488392>.
- Uz, Z., Ince, C., Rassam, F., Ergin, B., van Lienden, K.P., van Gulik, T.M., 2019. Assessment of hepatic microvascular flow and density in patients undergoing preoperative portal vein embolization. *HPB (Oxford)* 21, 187–194. <https://doi.org/10.1016/j.hpb.2018.07.002>.
- van der Horst, J., Siebers, A.G., Bulten, J., Massuger, L.F., de Kok, I.M., 2017. Increasing incidence of invasive and in situ cervical adenocarcinoma in the Netherlands during 2004–2013. *Cancer Med.* 6, 416–423. <https://doi.org/10.1002/cam4.971>.
- van Elteren, H.A., Ince, C., Tibboel, D., Reiss, I.K.M., de Jonge, R.C.J., 2015. Cutaneous microcirculation in preterm neonates: comparison between sidestream dark field (SDF) and incident dark field (IDF) imaging. *J. Clin. Monit. Comput.* 29, 543–548. <https://doi.org/10.1007/s10877-015-9708-5>.
- Vellinga, N.A.R., Boerma, E.C., Koopmans, M., Donati, A., Dubin, A., Shapiro, N.I., Pearse, R.M., Machado, F.R., Fries, M., Akarsu-Ayazoglu, T., Pranskunas, A., Hollenberg, S., Balestra, G., van Iterson, M., van der Voort, P.H.J., Sadaka, F., Minto, G., Aypar, U., Hurtado, F.J., Martinelli, G., Payen, D., van Haren, F., Holley, A., Pattnaik, R., Gomez, H., Mehta, R.L., Rodriguez, A.H., Ruiz, C., Canales, H.S., Duranteau, J., Spronk, P.E., Jhanji, S., Hubble, S., Chierago, M., Jung, C., Martin, D., Sorbara, C., Tijssen, J.G.P., Bakker, J., Ince, C., 2015. International study on microcirculatory shock occurrence in acutely ill patients. *Crit. Care Med.* 43, 48–56. <https://doi.org/10.1097/CCM.0000000000000553>.
- Walocha, J., Litwin, J., Bereza, T., Klimek-Piotrowska, W., Miodonski, A., 2012. Vascular architecture of human uterine cervix visualized by corrosion casting and scanning electron microscopy. *Hum. Reprod.* 27, 727–732. <https://doi.org/10.1093/humrep/der458>.
- Weber, M.A., Milstein, D.M.J., Ince, C., Oude Rengerink, K., Roovers, J.-P.W.R., 2015. Vaginal microcirculation: non-invasive anatomical examination of the micro-vessel architecture, tortuosity and capillary density. *NeuroUrol. Urodyn.* 34, 723–729. <https://doi.org/10.1002/nau.22662>.
- Weber, M.A., Milstein, D.M.J., Ince, C., Roovers, J.P.W.R., 2016. Is pelvic organ prolapse associated with altered microcirculation of the vaginal wall? *NeuroUrol. Urodyn.* 35, 764–770. <https://doi.org/10.1002/nau.22805>.
- Wiggins, D.L., Granai, C.O., Steinhoff, M.M., Calabresi, P., 1995. Tumor angiogenesis as a prognostic factor in cervical carcinoma. *Gynecol. Oncol.* 56, 353–356. <https://doi.org/10.1006/gyno.1995.1062>.